Journal of Zhejiang University-SCIENCE A (Applied Physics & Engineering)
ISSN 1673-565X (Print); ISSN 1862-1775 (Online)
www.zju.edu.cn/jzus; www.springerlink.com
E-mail: jzus@zju.edu.cn

Modeling natural convection heat transfer from perforated plates*

Zan WU, Wei LI, Zhi-jian SUN†‡, Rong-hua HONG
(*Department of Energy Engineering, Zhejiang University, Hangzhou 310027, China*)
†E-mail: zjsun@zju.edu.cn

Received Aug. 16, 2011; Revision accepted Feb. 10, 2012; Crosschecked Mar. 20, 2012

Abstract: Staggered pattern perforations are introduced to isolated isothermal plates, vertical parallel isothermal plates, and vertical rectangular isothermal fins under natural convection conditions. The performance of perforations was evaluated theoretically based on existing correlations by considering effects of ratios of open area, inclined angles, and other geometric parameters. It was found that staggered pattern perforations can increase the total heat transfer rate for isolated isothermal plates and vertical parallel plates, with low ratios of plate height to wall-to-wall spacing (*H*/*s*), by a factor of 1.07 to 1.21, while only by a factor of 1.03 to 1.07 for vertical rectangular isothermal fins, and the magnitude of enhancement is proportional to the ratio of open area. However, staggered pattern perforations are detrimental to heat transfer enhancement of vertical parallel plates with large *H*/*s* ratios.

Key words: Staggered pattern perforation, Natural convection, Inclined plate, Parallel plate, Rectangular fins
doi:10.1631/jzus.A1100222 **Document code:** A **CLC number:** TK01

1 Introduction

Buoyancy-driven ventilation appears in a variety of engineering applications, especially for cooling of electronic equipments and components. The main aim is to maintain a relatively constant component temperature to ensure system performance and reliability (Sugiura, 1997). For example, an excess temperature of high power light emitting diodes (LEDs) will cause decreases in luminous flux and maximum forward current, and deviations in color and forward voltage (Huh *et al.*, 2004). Thus, the fin industry has been engaged with the continuous search for an optimum geometry to achieve heat transfer enhancement (Bar-Cohen and Jelinek, 1985; Vollaro *et al.*, 1999; Baskaya *et al.*, 2000). In addition, numerical simulations were conducted to investigate heat transfer and flow pattern in parallel plates or fins (Morrone, 2001; Turgut and Onur, 2007).

One important method for heat transfer enhancement is to interrupt the temperature boundary layer by employing attachments, such as perforated holes. In the case of perforated attachments, the flow near the wall is interrupted repeatedly, increasing shear-induced mixing (turbulence). Apart from this, part of the improvement may be brought about by the multiple jet-like flows in the perforations. Despite the fact that correlations for natural convection within cavities and over the surfaces of non-perforated plates are readily available (Raithby and Hollands, 1984; Bejan, 2004), literature review indicated a scarcity of such relations for perforated surfaces. Sahin and Demir (2008) reported on heat transfer enhancement and the corresponding pressure drop over a flat surface equipped with square cross-sectional perforated pin fins in a rectangular channel. The optimum results were found to be Reynolds number (*Re*) of 42 000, fin height of 50 mm, and stream-wise distance between fins of 51 mm by the Taguchi experimental design method. Experiments were performed by Elshafei (2010) on natural convection heat transfer from circular pin fin sinks subjected to the influence of

‡ Corresponding author
* Project supported by the National Key Technology R&D Program of China (No. 2012BAA10B01), and the National Basic Research Program (973) of China (No. 2011CB710703)

geometry, heat flux, and orientation. The geometric dependence of heat dissipation of widely spaced solid and hollow/perforated circular pin fins with staggered combination, fitted into a heated base specifically. The heat transfer performance for heat sinks with hollow/perforated pin fins was better than that of solid pins. Al-Essa and Al-Hussien (2004) numerically investigated the effect of orientation of square perforation on the heat transfer enhancement from a single fin subjected to natural convection using the variational approach finite element technique. They found that the heat dissipation enhancement from a fin with square perforation parallel to its base was more than that of a fin with inclined square perforation, for a fin thickness larger than 2 mm.

Although some experimental and numerical investigations on perforated pin fins and isolated flat surface have been conducted, perforated attachments should be studied further to evaluate the potential of heat transfer enhancement on more structures when staggered pattern perforations are introduced with different ratios of open area. The present study aims to examine the extent of heat transfer enhancement from isolated isothermal perforated plates, vertical parallel isothermal perforated plates, and vertical rectangular isothermal perforated fins compared with their non-perforated counterparts with the same weight, under natural convection conditions. The performance of perforations was evaluated theoretically based on existing correlations by considering the effects of ratios of open area, inclined angles, and other geometric parameters. Because the studied plates or fins have the same plate or fin thickness and the same material, the same weight means that the perforated plates or fins and their non-perforated counterparts have the same surface area, without including the small area within perforations for perforated plates or fins.

2 Analyses and discussion

2.1 Assumptions

Considering the Murray-Gardner assumptions provided in (Kraus, 1988), the present study assumed the following conditions to simplify the analysis.

1. A steady state analysis is conducted for the heat flow and temperature distribution throughout the plate.

2. The plate material is homogeneous and isotropic.

3. There are no heat sources in the plate itself.

4. The thermal conductivity of the plate is constant.

5. The temperature of the surrounding fluid is uniform.

6. The temperature of the plate is uniform.

7. The thickness is so small compared to its height that temperature gradients normal to the surface may be neglected.

8. Side area of the plate is much smaller than its surface area.

9. Uniform heat transfer coefficient is over the whole solid surface.

10. Uniform heat transfer coefficient is within the perforation.

11. Radiation effects were neglected.

2.2 Isolated isothermal plate with staggered pattern perforations

A perspective view of a hollowed/perforated inclined plate is shown in Fig. 1. The range of the inclined angle θ is between 0° (a vertical plate) and 90° (a horizontal plate). The total heat transfer rate of the plate was calculated based on the unit length because plate length L>>plate height H. The rectangular perforations are introduced with a staggered pattern, as shown in Fig. 1b. The entire perforated plate consists of many of such patterns. In this analysis, the aspect ratio of the rectangular holes is a/b=2. All other dimensions are specified in Fig. 1. The open area ratio ε of the plate is defined as the ratio of cross-sectional area of perforations to that of the entire plate, which can be calculated approximately by

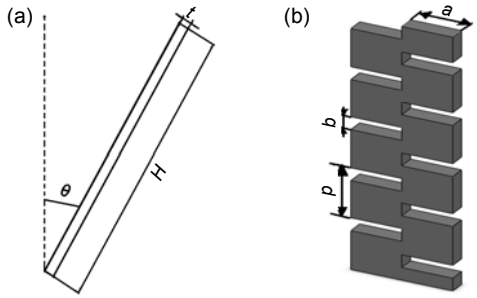

a: rectangular hole width; *b*: rectangular hole height; *H*: plate height; *p*: perforation pitch; *t*: plate thickness; *θ*: inclined angle

Fig. 1 Geometric parameters of an isolated inclined plate (a) with staggered pattern perforations (b)

$$\varepsilon = \mathrm{int}\left(\frac{H}{p}\right)\cdot \mathrm{int}\left(\frac{1}{a}\right)\cdot\frac{ab}{H} < \frac{1}{2}, \tag{1}$$

where a, b, and p denote the rectangular hole width, rectangular hole height, and perforation pitch, respectively. That $\varepsilon<1/2$ is because p must be larger than $2b$ for staggered pattern perforations.

The total heat transfer rate of the inclined perforated plate q_{h} consists of two parts: heat rate q_{hs} from the remaining peripheral surface area with heat transfer coefficient of h_{hs}, and heat rate from the perforation inner lining surface q_{hc} with heat transfer coefficient of h_{hc}. Eq. (2) is introduced to estimate h_{hs} in terms of ratio of the open area ε and h_{s} (heat transfer coefficient of a non-perforated plate) as provided by Al-Essa and Al-Hussien (2004):

$$h_{\mathrm{hs}} = (1+0.75\varepsilon)h_{\mathrm{s}}, \tag{2}$$

where $(1+0.75\varepsilon)$ is called the heat transfer augmentation ratio of the interrupted surface. The wall-averaged value of h_{s} for a vertical isothermal plate in natural convection was calculated using the correlation proposed by Churchill and Chu (1975) for the entire Rayleigh number range (laminar, transition, and turbulent):

$$Nu_{\mathrm{v}} = \frac{h_{\mathrm{s}}L_{\mathrm{c}}}{k_{\mathrm{air}}} = \left\{0.825 + \frac{0.387Ra^{1/6}}{\left[1+(0.492/Pr)^{9/16}\right]^{8/27}}\right\}^2, \tag{3}$$

$$10^{-1} < Ra < 10^{12},$$

$$Ra = \frac{g\beta(T_{\mathrm{w}}-T_{\infty})L_{\mathrm{c}}^3}{\alpha\nu}, \tag{4}$$

where Nu_{v} is the Nusselt number of the vertical plate, L_{c} is the characteristic length, k_{air} is the thermal conductivity of air, Ra is the Rayleigh number, Pr is the Prandtl number, g is the gravitational acceleration, β is the coefficient of thermal expansion, T_{w} is the wall temeprature, T_{∞} is the ambient temperature, α is the thermal diffusivity, and ν is the kinematic viscosity.

For inclined plates with $0<\theta\leq60°$, it is found that the momentum equation is analogous to that of vertical plates, except that $g\cos\theta$ replaces g in the buoyancy term according to Bejan (2004). The term $g\cos\theta$ is the gravitational acceleration component that is oriented parallel to the wall. For this reason, in the laminar regime, the heat transfer rate along an inclined isothermal wall with $0<\theta\leq60°$ can be calculated with Eq. (3), provided that the Rayleigh number Ra is based on $g\cos\theta$:

$$Ra_i = \frac{g\cos\theta\cdot\beta(T_{\mathrm{w}}-T_{\infty})L_{\mathrm{c}}^3}{\alpha\nu}. \tag{5}$$

For vertical and inclined plates, L_{c} equals to the height H. In the turbulent regime, Bejan (2004) found that the heat transfer measurements are correlated better using g than $g\cos\theta$ in the Rayleigh number group when $0<\theta<90°$.

The upper surface of a horizontal isothermal plate ($\theta=90°$) is hot and faces upward, the flow leaves the boundary layer as a vertical plume rooted in the central part of the wall. The general Nusselt number for this kind of upper surface Nu_{us} varies as

$$Nu_{\mathrm{us}} = \frac{h_{\mathrm{s}}L_{\mathrm{c}}}{k_{\mathrm{air}}} = (Nu_{\mathrm{l}}^{10} + Nu_{\mathrm{t}}^{10})^{1/10}$$
$$= \left\{\left[1.4\Big/\ln\left(1+\frac{1.4}{\overline{C_{\mathrm{l}}}Ra^{1/4}}\right)\right]^{10} + \left(0.14Ra^{1/3}\right)^{10}\right\}^{1/10}, \tag{6}$$

$$\overline{C_{\mathrm{l}}} = \frac{4}{3}\cdot\frac{0.503}{\left[1+(0.492/Pr)^{9/16}\right]^{4/9}}, \tag{7}$$

where Nu_{us} is the upper surface Nusselt number, Nu_{l} and Nu_{t} are the Nusselt number in the laminar regime and the turbulent regime, respectively. The Rayleigh number Ra is calculated by Eq. (4). For horizontal plates, characteristic length L_{c} of the plane surface is defined as

$$L_{\mathrm{c}} = \frac{\text{heated area}}{\text{heated perimeter}} = \frac{HL}{2(H+L)} \approx \frac{H}{2},\ L >> H. \tag{8}$$

Considering the lower surface of a horizontal isothermal plate, which is heated and faces downward, the boundary layer covers the entire surface, and the flow "spills" over the side edges. Thus, the heat transfer rate of the lower surface is less than that of the upper surface. Because the stabilizing effect of the heated surface results in laminar flow up to a very

high Rayleigh number, the turbulence effect is neglected in the corresponding correlation for hot surface facing downward:

$$Nu_{ls}=\frac{h_s L_c}{k_{air}}=\frac{0.527}{\left[1+(1.9/Pr)^{9/10}\right]^{2/9}}Ra^{1/5}, \quad (9)$$

where Nu_{ls} is the lower surface Nusselt number.

For an inclined plate with $60°<\theta<90°$ in the laminar regime, the recommended procedure is to calculate the Nusselt number from Eqs. (3) and (5) and the Nu_l in Eq. (6) for $\theta=90°$, and to use the maximum of these two values.

In the above equations, only the coefficient of thermal expansion β is evaluated at the ambient temperature T_∞. Other physical properties are evaluated at the film temperature $(T_w+T_\infty)/2$. From h_s, h_{hs} can be obtained using Eq. (2). The total heat transfer rate for non-perforated plate q_s is the product of h_s and corresponding heat transfer surface area.

For vertical perforations, heat transfer coefficient h_{hc} is calculated by the following equations according to Raithby and Hollands (1984):

$$Nu_{hc}=\frac{h_{hc}L_c}{k_{air}}=\left[\left(\frac{Ra_{hc}}{15.55}\right)^{-1.5}+(0.62Ra_{hc}^{1/4})^{-1.5}\right]^{\frac{1}{-1.5}},$$

$$Ra_{hc}<10^4, \quad (10)$$

$$L_c=\frac{2A}{P}=\frac{ab}{a+b}, \quad (11)$$

$$Ra_{hc}=\frac{g\beta(T_w-T_\infty)L_c^3}{\alpha\nu}\cdot\frac{L_c}{t}, \quad (12)$$

where Nu_{hc} is the Nusselt number of the perforations, t the plate thickness, A is the heat transfer area, and P is the perimeter.

For inclined perforations, Ra_{hc} is replaced by $Ra_{hc}\sin\theta$ in Eq. (10). The heat transfer rate for perforated plate q_h can be obtained as

$$q_h=q_{hs}+q_{hc}$$
$$=(T_w-T_\infty)$$
$$\times\left[(1-\varepsilon)H\cdot h_{hs}+\mathrm{int}\left(\frac{H}{p}\right)\cdot\mathrm{int}\left(\frac{1}{a}\right)\cdot 2(a+b)t\cdot h_{hc}\right]. \quad (13)$$

Heat transfer comparisons between isolated perforated plate and non-perforated plate as a function of the plate height were presented in Fig. 2. The ratio of heat transfer rate for perforated plate with staggered pattern to non-perforated plate (q_h/q_s) is evaluated at the same weight of the perforated and non-perforated plates. The ratio q_h/q_s increases with plate height H for different inclined angles at $\varepsilon=0.25$. The rate of increase decreases gradually with H. Perforated holes can increase the total heat transfer rate by a factor of 1.08 to 1.16. This can be attributed to the fact that the wall-averaged heat transfer coefficient of the region $H<0.6$ decreases with Ra greater than that of the region $H>0.6$. When $0°\leq\theta\leq60°$, trends of the three curves are similar. However, the trend of horizontal plate ($\theta=90°$) is steeper than the other three. The ratio of q_h/q_s is lower than that of inclined plates when $H<0.7$; after that q_h/q_s becomes larger than that of inclined plates.

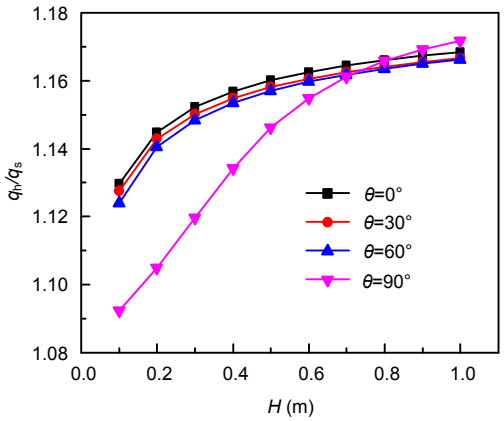

Fig. 2 Ratio of heat transfer rate for isolated perforated plate to non-perforated plate (q_h/q_s) as a function of the plate height at various inclined angles, ε=0.25, and t=0.002 m

Fig. 3 presents the relationship between heat transfer rate q and ratio of open area ε. Heat transferred by the perforated plate q_h decreases with an increase in ε. Although average heat transfer coefficient increases with ε, its contribution to heat increase is less than the heat decrease caused by the reduction in total heat transfer area. Because the equivalent H for non-perforated plate decreases with ε, the heat transfer rate decrease also results from the decrease of surface area. It is also apparent from Fig. 3 that the q_h/q_s ratio becomes larger at a larger ε. As a result, it can be inferred that the enhancement of heat transfer

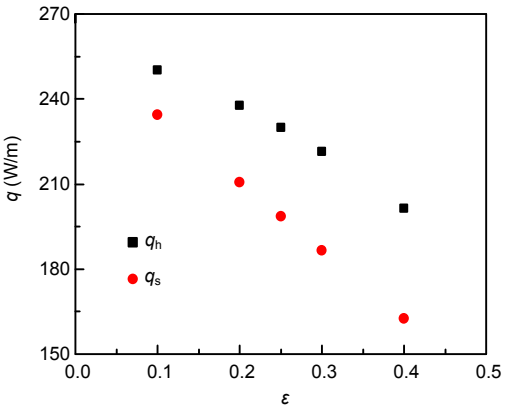

Fig. 3 Heat transfer rate vs ratio of open area for perforated and non-perforated isolated plates with the same weight, H=0.5 m, t=0.002 m, and θ=30°

is linearly dependent on ε compared with its non-perforated counterpart at the same weight, however, with a decrease in total heat transfer rate.

2.3 Vertical parallel isothermal plates with staggered pattern perforations

As illustrated in Fig. 4a with a relatively high H/s ratio, boundary layers of the two facing sides will merge into a single buoyant stream rising through the chimney formed by the two walls, typical of a fully developed region (i.e., velocity and temperature profiles become invariant with distance along the channel). The Nusselt number for this kind of vertical parallel plates can be calculated by

$$Nu_{\mathrm{fd}}=\frac{h_s s}{k_{\mathrm{air}}}=\frac{Ra_{\mathrm{vp}}}{fRe}, \tag{14}$$

$$Ra_{\mathrm{vp}}=\frac{g\beta(T_{\mathrm{w}}-T_{\infty})s^3}{\alpha\nu}\cdot\frac{s}{H}, \tag{15}$$

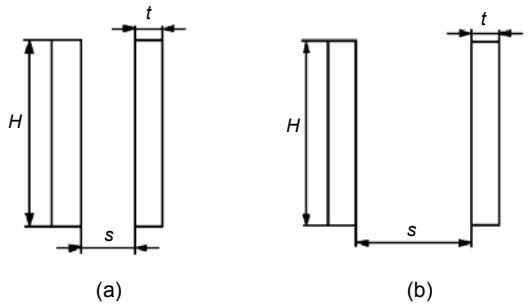

Fig. 4 Geometric parameters of vertical parallel isothermal plates with high (a) and low (b) H/s ratios

where Nu_{fd} is the fully developed Nusselt number, s is the wall-to-wall spacing, and fRe is the friction factor-Reynolds number product, which depends on duct shapes. For the case a/b=2 in analysis, fRe=15.55. The relationship of the fully developed Nusselt number to fRe was originally pointed out by Elenbass (1942). When Ra_{vp} approaches zero, Martin *et al.* proposed a more accurate correlation as reported in (Bejan, 2004):

$$Nu_{\mathrm{fd}}=\frac{h_s s/2}{k_{\mathrm{air}}}=\frac{Ra_{\mathrm{vp}}}{6(H/b)}\left[1+\sqrt{1+\frac{12}{(H/b)Ra_{\mathrm{vp}}}}\right], \tag{16}$$

$$Ra_{\mathrm{vp}}=\frac{g\beta(T_{\mathrm{w}}-T_{\infty})(s/2)^3}{\alpha\nu}\cdot\frac{s/2}{H}. \tag{17}$$

However, the fully developed flow and heat transfer solutions break down if the following inequality given by Bejan (2004) is valid:

$$(Ra\cdot Pr)^{\frac{1}{4}}=\left[\frac{g\beta(T_{\mathrm{w}}-T_{\infty})H^3}{\alpha^2}\right]>2\left(\frac{H}{s}\right)^{\frac{1}{4}}. \tag{18}$$

In this case, the boundary layer thickness scales are much smaller than the wall-to-wall spacing s. The flow along one wall may be regarded as a wall jet unaffected by the presence of another wall, as demonstrated in Fig. 4b. In the latter case, the heat transfer relation is similar in form to that for a vertical plate, but the heat transfer is usually measured to be higher, which is thought to result from the flow induced through the cavity by the chimney effect. Aung (1972) proposed a general correlation for different H/s ratios:

$$Nu_{\mathrm{vp}}=\frac{h_s s}{k_{\mathrm{air}}}=\left[Nu_{\mathrm{fd}}^{-1.9}+(0.62Ra_{\mathrm{vp}}^{1/4})^{-1.9}\right]^{\frac{1}{-1.9}}, \tag{19}$$

where Nu_{vp} is the Nusselt number of the vertical plate. For perforated plates with the same staggered pattern illustrated in Fig. 1, the heat transfer coefficient of h_{hs} for the remaining peripheral surface area was also calculated by Eq. (2).

For relatively high H/s ratios, $q_{\mathrm{h}}/q_{\mathrm{s}}$ is less than unity for different ratios of open area and wall-to-wall spacing, as demonstrated in Fig. 5a. The value of $q_{\mathrm{h}}/q_{\mathrm{s}}$

is larger for higher ratio of open area. This suggests that perforated holes are harmful for heat transfer enhancement of vertical parallel plates with H/s ratios larger than $(Ra{\cdot}Pr)^{1/4}$. This is because the heat transfer coefficient of parallel perforated plates is less than that of non-perforated parallel plates with the same weight. However, for relatively low H/s ratios, the values of q_h/q_s are about 1.04 and 1.12 when ε=0.05 and 0.25, respectively (Fig. 5b). Therefore, perforations can enhance heat transfer for vertical parallel plates with H/s ratios less than $(Ra{\cdot}Pr)^{1/4}$.

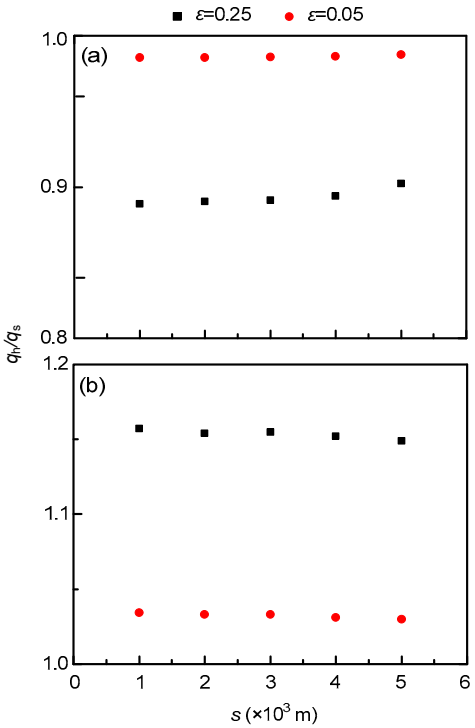

Fig. 5 Ratio of heat transfer rate of high (a) and low (b) H/s ratios perforated to non-perforated vertical parallel plates with the same weight vs wall-to-wall spacing for different ratios of open area, t=0.002 m

2.4 Vertical rectangular isothermal perforated fins on vertical surfaces

Fig. 6 presents vertical rectangular perforated fins. If $W/s\geq 5$ (W is the fin width), the Nusselt number is essentially the same as for the parallel-plate channel (Raithby and Hollands, 1984). Also, as W/s approaches zero, the heat transfer should approach that for a vertical flat plate. Van De Pol and Tierney proposed the following equation for $0.6<Ra<100.0$, Pr=0.71 (air), $0.33<W/s<4.00$, and $0.42<H/s<10.60$ as reported in (Raithby and Hollands, 1984):

$$Nu=\frac{Ra_{vf}}{\Psi}\left\{1-\exp\left[-\Psi\left(\frac{0.5}{Ra_{vf}}\right)^{3/4}\right]\right\}, \tag{20}$$

$$Ra_{vf}=\frac{g\beta(T_w-T_\infty)L_c^3}{\alpha\nu}\cdot\frac{L_c}{H}, \tag{21}$$

$$L_c=2Ws/(2W+s), \tag{22}$$

$$\Psi=24(1-0.483e^{-0.17W/s})\cdot\left\{1+0.5\frac{s}{W}\times\left[1+(1-e^{-0.83s/W})\cdot\left(9.14\sqrt{\frac{s}{W}}\cdot e^{-0.0465s}-0.61\right)\right]\right\}^{-3}. \tag{23}$$

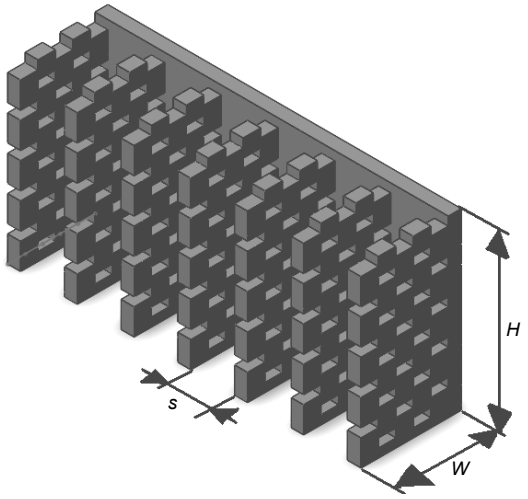

Fig. 6 Vertical rectangular isothermal perforated fins on vertical surfaces

As shown in Fig. 7, for the same ε, q_h/q_s are nearly equal. There is only a slight increase with H/s. For the same H/s, q_h/q_s increases with ε. However, for the same ε, enhancement of heat transfer is less efficient than that for isolated isothermal perforated plate. For example, when ε=0.40, q_h/q_s is approximately equal to 1.21 for isolated perforated plate, while q_h/q_s is about 1.07 for vertical rectangular isothermal perforated fins.

3 Conclusions

The present study examined the extent of heat transfer enhancement from isolated isothermal perforated plates with staggered patterns, vertical parallel isothermal perforated plates, and vertical

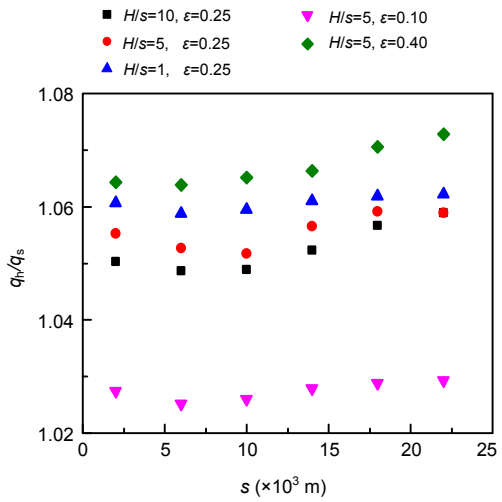

Fig. 7 Ratio of heat transfer rate of perforated to non-perforated vertical rectangular isothermal fins with the same weight vs wall-to-wall spacing at various *H*/*s* and ratios of open area, *t*=0.002 m

rectangular isothermal perforated fins compared with their non-perforated counterparts with the same weight by using existing correlations, under natural convection conditions. Most of the correlations were adopted for calculating h_s under different conditions. However, the q_h/q_s ratio is almost unaffected by the uncertainties of these correlations, because the h_s value is also present in q_h term and accounts for a large amount of q_h. The q_h/q_s ratio has a similar level of uncertainty with Eq. (2) resulting from the term $(1+0.75\varepsilon)$, the heat transfer augmentation ratio of the interrupted surface which should be experimentally and numerically investigated comprehensively in the future. The following points were concluded from the above analyses:

1. Perforations can enhance heat transfer for isolated isothermal plate, vertical parallel plates with low *H*/*s* ratios, and vertical rectangular fins with dimensions specified in Section 2.4.

2. When $0.10\leq\varepsilon\leq0.40$, perforated holes can increase the total heat transfer rate for isolated isothermal plate and vertical parallel plates with low *H*/*s* ratios by a factor of 1.07 to 1.21, while only by a factor of 1.03 to 1.07 for vertical rectangular isothermal fins. The magnitude of enhancement is proportional to the ratio of open area ε.

3. The ratio of q_h/q_s is relatively independent of the inclined angle θ.

4. For relatively high *H*/*s* ratios, q_h/q_s is less than 1 for different ratios of open areas and wall-to-wall spacing. Thus, perforated holes are harmful for heat transfer enhancement of vertical parallel plates with $H/s>(Ra\cdot Pr)^{1/4}$.

Acknowledgements

The first author Mr. Zan WU would like to appreciate the WU Zhong-hua Fund for excellent graduate students in China.

References

Al-Essa, A.H., Al-Hussien, F.M.S., 2004. The effect of orientation of square perforations on the heat transfer enhancement from a fin subjected to natural convection. *Heat and Mass Transfer*, **40**(6-7):509-515. [doi:10.1007/s00231-003-0450-z]

Aung, W., 1972. Fully developed laminar free convection between vertical plates heated asymmetrically. *International Journal of Heat and Mass Transfer*, **15**(8):1577-1580. [doi:10.1016/0017-9310(72)90012-9]

Bar-Cohen, A., Jelinek, M., 1985. Optimum arrays of longitudinal, rectangular fins in convective heat transfer. *Heat Transfer Engineering*, **6**(3):68-78. [doi:10.1080/01457638508939633]

Baskaya, S., Sivrioglu, M., Ozek, M., 2000. Parametric study of natural convection heat transfer from horizontal rectangular fin arrays. *International Journal of Thermal Sciences*, **39**(8):797-805. [doi:10.1016/S1290-0729(00)00271-4]

Bejan, A., 2004. Convection Heat Transfer, 3rd Edition. John Wiley & Sons, Inc., New York, p.178-242.

Churchill, S.W., Chu, H.H.S., 1975. Correlating equations for laminar and turbulent free convection from a vertical plate. *International Journal of Heat and Mass Transfer*, **18**(11):1323-1329. [doi:10.1016/0017-9310(75)90243-4]

Elenbass, W., 1942. The dissipation of heat by free convection: the inner surface of vertical tubes of different shapes of cross-section. *Physica*, **9**(8):865-874. [doi:10.1016/S0031-8914(42)80062-2]

Elshafei, E.A.M., 2010. Natural convection heat transfer from a heat sink with hollow/perforated circular pin fins. *Energy*, **35**(7):2870-2877. [doi:10.1016/j.energy.2010.03.016]

Huh, C., Schaff, W.J., Eastman, L.F., Park, S.J., 2004. Temperature dependence of performance of InGaN/GaN MQW LED switch different indium compositions. *IEEE Electron Device Letters*, **25**(2):61-63. [doi:10.1109/LED.2003.822659]

Kraus, A.D., 1988. Sixty-five years of extended surface technology (1922–1987). *Applied Mechanics Reviews*, **41**(9):321-364. [doi:10.1115/1.3151910]

Morrone, B., 2001. Natural convection between parallel plates with conjugate conductive effects. *Numerical Heat Transfer, Part A: Applications*, **40**(8):873-886. [doi:10.1080/104077801753344312]

Raithby, G.D., Hollands, K.G.T., 1984. Natural Convection. *In*: Rohsenow, W., Hartnett, J., Ganic, E. (Eds.), Handbook of Heat Transfer Fundamentals, 2nd Edition. McGraw-Hill Book Company, New York, p.1-94.

Sahin, B., Demir, A., 2008. Performance analysis of a heat exchanger having perforated square fins. *Applied Thermal Engineering*, **28**(5-6):621-632. [doi:10.1016/j.applthermaleng.2007.04.003]

Sugiura, L., 1997. Dislocation motion in GaN light-emitting devices and its effect on device lifetime. *Journal of Applied Physics*, **81**(1):633-638. [doi:10.1063/1.364018]

Turgut, O., Onur, N., 2007. An experimental and three-dimensional numerical study of natural convection heat transfer between two horizontal parallel plates. *International Communications in Heat and Mass Transfer*, **34**(5):644-652. [doi:10.1016/j.icheatmasstransfer.2007.02.001]

Vollaro, A.L., Grignaffini, S., Gugliermetti, F., 1999. Optimum design of vertical rectangular fin arrays. *International Journal of Thermal Sciences*, **38**(6):525-529. [doi:10.1016/S1290-0729(99)80025-8]